

Neuroprotection of *Cyperus esculentus* L. orientin against cerebral ischemia/reperfusion induced brain injury

Si-Qun Jing^{1,*}, Sai-Sai Wang², Rui-Min Zhong¹, Jun-Yan Zhang¹, Jin-Zi Wu³, Yi-Xian Tu⁴, Yan Pu⁴, Liang-Jun Yan^{3,*}

¹ Yingdong College of Food Science and Engineering, Shaoguan University, Shaoguan, Guangdong Province, China

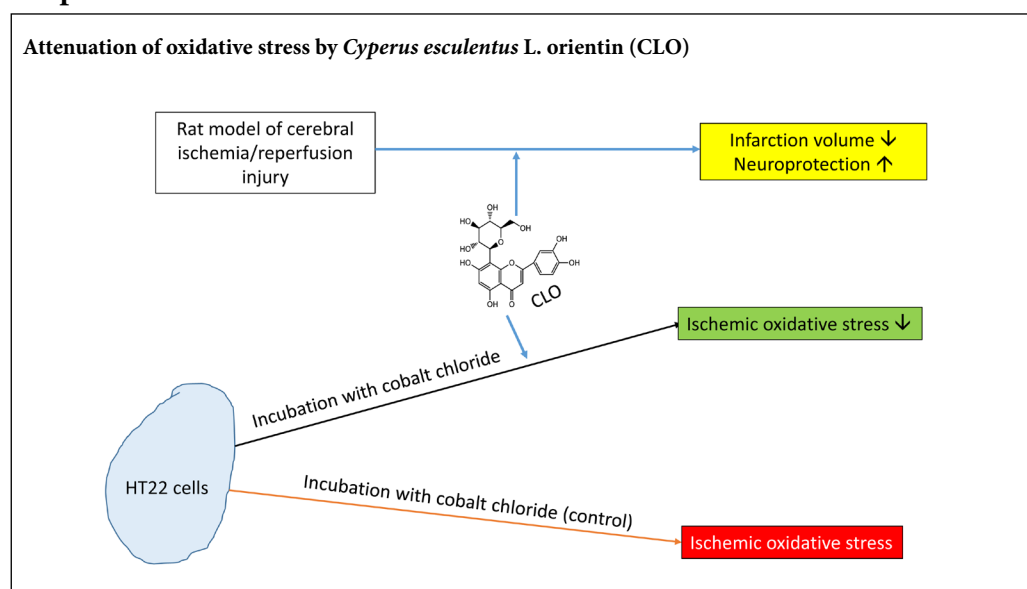
² School of Bioengineering, Jiangnan University, Wuxi, Jiangsu Province, China

³ Department of Pharmaceutical Sciences, UNT System College of Pharmacy, University of North Texas Health Science Center, Fort Worth, TX, USA

⁴ College of Life Sciences and Technology, Xinjiang University, Urumqi, Xinjiang Uygur Autonomous Region, China

Funding: This work was supported by the National Natural Science Foundation of China, No. 31770385 (to SQJ).

Graphical Abstract



***Correspondence to:**

Si-Qun Jing, PhD,
jingsiqun@163.com;
Liang-Jun Yan, PhD,
liang-jun.yan@unthsc.edu.

orcid:

0000-0002-2937-3594
(Si-Qun Jing)
0000-0002-5815-5430
(Liang-Jun Yan)

doi: 10.4103/1673-5374.266063

Received: February 18, 2019

Accepted: June 18, 2019

Abstract

Orientin is a flavonoid monomer. In recent years, its importance as a source of pharmacological active substance is growing rapidly due to its properties such as anti-myocardial ischemia, anti-apoptosis, anti-radiation, anti-tumor, and anti-aging. However, the neuroprotective effects of Orientin on stroke injury have not been comprehensively evaluated. The aim of the present study was thus to investigate the neuroprotective capacity and the potential mechanisms of *Cyperus esculentus* L. orientin (CLO) from *Cyperus esculentus* L. leaves against ischemia/reperfusion (I/R) injury using standard orientin as control. For *in vitro* studies, we treated HT22 cells with CoCl₂ as an *in vitro* ischemic injury model. HT22 cells in the control group were treated with CoCl₂. For *in vivo* studies, we used rat models of middle cerebral artery occlusion, and animals that received sham surgery were used as controls. We found that CLO protected CoCl₂-induced HT22 cells against ischemia/reperfusion injury by lowering lipid peroxidation and reactive oxygen species formation as well as decreasing protein oxidation. However, CLO did not reduce the release of lactate dehydrogenase nor increase the activity of superoxide dismutase. Results showed that CLO could decrease neurological deficit score, attenuate brain water content, and reduce cerebral infarct volume, leading to neuroprotection during cerebral ischemia-reperfusion injury. Our studies indicate that CLO flavonoids can be taken as a natural antioxidant and bacteriostatic substance in food and pharmaceutical industry. The molecular mechanisms of CLO could be at least partially attributed to the antioxidant properties and subsequently inhibiting activation of caspase-3. All experimental procedures and protocols were approved on May 16, 2016 by the Experimental Animal Ethics Committee of Xinjiang Medical University of China (approval No. IACUC20160516-57).

Key Words: antioxidants; caspase-3; cerebral ischemia/reperfusion injury; cobalt chloride; *Cyperus esculentus* L. orientin (CLO); lipid peroxidation; nerve regeneration; neurological deficits; oxidative stress; reactive oxygen species

Chinese Library Classification No. R453; R363; R364

Introduction

Cyperus esculentus L. (*Cyperus esculentus* L. Var. *Sativus* Baeck) belongs to the Cyperaceae family, which is a C3 sedge genus perennial herb that can be used as oil plants and fine pasture (Ayeih-Kumi et al., 2014) and is also known as tigernut, earth nuts, earth almond, rush nuts, and chufas. *C. esculentus* L. originates from the Mediterranean Coast in North Africa, and mainly includes three parts: underground tubers, roots, and leaves above the ground. It was described in an ancient Chinese medical book, *Min-Yi-Bie-Lu* that *C. esculentus* L. leaves can be applied to ease some symptoms, such as depression, wind-dispelling and itching, discomfort and fullness in the chest. Our research group has confirmed that the effective components in *C. esculentus* L. leaves contain flavonoids that have various biological activities, such as anti-oxidative effects *in vitro* and *in vivo*, anti-bacterial function, promoting blood microcirculation, and anticoagulant effect (Jing et al., 2016). Moreover, we have recently reported that *C. esculentus* L. extract exhibits beneficial effects on microcirculation and anticoagulation property (Su et al., 2017). The specimen for the extract investigated in this study was deposited in Herbarium of Xinjiang University, collected on October 15, 2017 from Qiemo County, Bazhou District, Xinjiang Uyghur Autonomous Region, China.

Flavonoids, belonging to the polyphenol family, are secondary metabolites of plants and can exert important physiological and biochemical effects due to their unique chemical structures. It has been reported that flavonoids can decrease the incidence of cancer, diabetes, and cardiovascular disease (Xia et al., 2014). Orientin is a flavonoid monomer, mainly in *trollius chinensis* bunge, *lindsaea* spp., *phyllostachys*, *patrinia villosa* juss, *indocalamus latifolius* (keng) and other medicinal plants. In recent years, their importance as a source of pharmacological active substances is growing rapidly due to its properties such as anti-myocardial ischemia, anti-apoptosis, anti-radiation, anti-tumor, anti-aging and other biological effects (Liu et al., 2016). It is believed that the biological mechanism is mainly due to antioxidation.

Ischemic stroke, which makes up more than 80% of stroke, remains a leading cause of adult disability and death (Lee et al., 2017; Chang et al., 2018; Li et al., 2019). Mechanisms of stroke injury include glutamate excitotoxicity, calcium overload, oxidative stress, and apoptosis (Simoes Pires et al., 2014; Li et al., 2018). Indeed, oxidative stress has been reported to play a critical role in the pathological mechanisms of ischemic stroke (Feng et al., 2016; Zhang et al., 2017). When beyond the capacity of antioxidant systems, excessive free radicals trigger numerous molecular and cellular cascades to mediate inflammation and cell death, subsequently inducing blood-brain barrier (BBB) hyperpermeability, brain edema, and infarction enlargement (Chan, 2001). Many antioxidants, such as edaravone and N-acetylcysteine (NAC), protect nerve cells against cerebral ischemia/reperfusion injury (Pun et al., 2009). Flavonoids exert protective effects mainly through mechanisms involving anti-inflammatory and antioxidant properties and modulating lipid metabolism and platelet function (Gao et al., 2001; Chun et al., 2008; Weseler and

Bast, 2012; Goszcz et al., 2017; Tokmak et al., 2017). However, there is little information on the protective effects of flavonoids monomer Orientin isolated from *Cyperus esculentus* L. leaves (CLO) on cerebral ischemia/reperfusion (I/R) injury, especially on hippocampal neuronal cells. Given that oxidative stress play important roles in cerebral I/R injury and flavonoid has antioxidant properties, we hypothesize in the present study that CLO flavonoid could protect against cerebral I/R injury through inhibiting oxidative stress mediated neuronal apoptosis.

Materials and methods

In vitro cell culture

Mouse HT22 cell line is a neuronal cell and was received as a generous gift from Dr. Wen-Jun Li from the University of North Texas Health Scientific Center (Fort Worth, USA).

Extraction and isolation of plant material

Standard orientin (STO; Lot Number: 111777-201302, CAS: 28608-75-5) was purchased from National Institutes for Food and Drug Control. Flavonoids monomer of CLO was isolated from the leaves of *Cyperus esculentus* L. in our own laboratory. The dried and milled plant material (1200 g) was extracted with 50% and 95% EtOH three times by maceration. The extracts were combined and concentrated in vacuole at 50°C to give the 50% and 95% EtOH extract. Fifty percent and 95% EtOH extracts (129.972 g) were suspended in deionized water and successively eluted with EtOH at different concentration gradients (0, 30%, 50%, 70%, and 95%) respectively. Based on the DPPH (1,1-diphenyl-2-picryl-hydrazyl) radical scavenging activities of different fractions, we chose the 30% EtOH extracts for detailed phytochemical investigation. A portion of the 30% EtOH extract was chromatographed over reverse phase silica gel (5 cm × 20 cm, 50 mesh) and Sephadex LH-20 column [2 × (60–80 cm)], eluted with EtOH gradients, based on thin layer chromatography analysis. After monomeric compounds were obtained, the monomer structure was identified by nuclear magnetic resonance (NMR) technology.

In vivo experimental cerebral ischemia/reperfusion models and drug treatment

A total of 72 young adult male Sprague-Dawley rats weighing 250–300 g (8–10 weeks old) were obtained from the medical laboratory animal center of Xinjiang Medical University, with the license number of the use of experimental animals: SCXK (Xin) 2011-0004. All experimental procedures and protocols were approved on May 16, 2016 by the Experimental Animal Ethics Committee of Xinjiang Medical University of China (approval No. IACUC20160516-57). Rats were fed ad libitum with 12-hour light/dark cycle in the colony room. The experimental procedure followed the United States National Institutes of Health Guide for the Care and Use of Laboratory Animals (NIH Publication No. 85-23, revised 1996).

The experimental procedures and protocols were approved by the local legislations for ethics of animal experiments.

Each group contained 12 rats. For ischemia reperfusion, focal cerebral ischemia was induced by the middle cerebral artery occlusion (MCAO) method (Longa et al., 1989; Duan et al., 2015). Briefly, after anesthesia, the left common carotid artery (CCA), internal carotid artery (ICA), and external carotid artery (ECA) were exposed through a midline incision of the neck. A 3–10 silica gel-coated nylon suture was used as an embolus and inserted to the origin of middle cerebral artery (MCA) via the ECA to block the MCA and then the suture was withdrawn for reperfusion. In sham-operated animals, the suture was inserted 5 mm from the incision and no cerebral ischemia was induced as confirmed by ultrasound detection. After the operation, animals were transferred into an intensive care chamber with temperature maintained at 37°C until animals woke up completely. Successful ischemic reperfusion model was assessed by histochemical staining of brain infarction volume.

Sprague-Dawley rats were randomly divided into six groups, including sham group, model group (the above two groups were given the same volume of distilled water), positive control group 1 (nimodipine solution 20 mg/kg, Sigma, St. Louis, MO, USA), positive control group 2 (gingko leaf blade 0.3 mg/kg (double dosage of clinical use), *C. esculentus* L. 30% elution high-dose intervention group (500 mg/kg), *C. esculentus* L. 30% elution low-dose intervention group (125 mg/kg). Rats in each group underwent intragastric administration at a designated dose for 7 days, with a volume of 10 mL/kg, followed by stroke surgery on day 8 after 0.5 hours of the last dose.

***In vivo* experiment**

Neurological deficit score

According to the method of Longa (Longa et al., 1989), animal's performance was scored after anesthesia at the end of 24 hours of reperfusion and neurological deficit symptoms were recorded ($n = 6$ rats/group). The Longa scoring criteria were as follows: a score of 0, no neurologic deficit; 1, failure to extend contralateral forepaw fully when the tail was raised; 2, bend the contralateral forepaw when the tail was raised; 3, turn to the paralyzed side when walking; 4, turn to the paralysis seriously when walking.

Brain water content measurement

Brain water content was measured immediately after 24 hours of reperfusion. Six rats of each group were decapitated and the brain was removed quickly.

The wet weight and dry weight of two cerebral hemispheres were measured before and after drying in a 160°C oven for 24 hours respectively. Brain water content was calculated according to the formula: brain water content (%) = (wet weight – dry weight)/wet weight \times 100%.

Infarct volume measurement

Infarct volume was measured immediately after 24 hours reperfusion. Six rats from each group were decapitated, the brains were removed immediately, cut into 2 mm-thick coronal slices, and incubated for 30 minutes in 2% 2,3,5-triph-

enyltetrazolium chloride (TTC) solution at 37°C. The infarct area was white and the non-infarct area was red. Digital camera was used to measure the total volume of brain slices and the volume of infarct area with Medbrain 2.0 software (Nanjing Meiyi Technology Company, China). The percentage of infarct area in the whole brain tissue was calculated (%).

***In vitro* experiment**

Cell culture

The mouse hippocampal neuronal cell line, HT22 cells, were maintained in DMEM supplemented with 10% (v/v) FBS and 1% antibiotics (penicillin/streptomycin) and were incubated in a humidified incubator overnight at 5% CO₂ at 37°C prior to use. Each cell line was sub-cultured every 2 or 3 days. Cells were harvested and 1×10^4 cells/well were incubated in a 96-well plate or 3×10^5 cells/well in a 6-well plate. The culture medium was changed every other day. The growth condition and morphological changes of cells were observed and photographed with an inverted microscope (EVOS XL Cell Imaging System, San Diego, CA, USA).

Cell treatment

HT22 cells were randomly divided into 10 groups ($n = 6$ per group): a CoCl₂ group (CoCl₂) as the model group, a normal control group (Con), four CLO and four STO groups (100, 200, 400, and 600 μ g/mL). STO was administered 4 hours after reperfusion. The dose chosen in this study was based on our preliminary studies. In the CLO and STO groups, HT22 cells were incubated with different concentrations of CLO and STO. *In vitro* ischemia and reperfusion treatment were performed as described previously (Yang et al., 2015). HT22 cells in the CoCl₂ group were incubated with 500 μ M CoCl₂ (Sigma) for 16 hours and culture medium was removed thereafter. Meanwhile, DMEM with 10% FBS were added. The control group was treated with DMEM with 10% FBS and was maintained under the same conditions.

WST-8 assay for cell viability and cytotoxicity

All measurements were performed after 16 hours of CoCl₂ treatment and 4 hours of reperfusion (the same below for lactate dehydrogenase (LDH) assay, superoxide dismutase (SOD), reactive oxygen species (ROS), protein carbonyl and apoptosis). Cell viability and cytotoxicity assay were measured with WST-8 dye according to the instructions of the manufacturers. In brief, HT22 cells were plated in 96-well plates at a density of 1×10^4 cells per well as described above. Six wells were prepared for each treatment or control. Ten microliter of the tetrazolium salt WST-8 solution was added to each well of the 96-well plate containing 100 μ L of fresh DMEM medium and incubated for 2 hours at 37°C. The absorbance was detected at 450 nm using BioTek's Gen5™ Microplate Readers (BioTek, Winooski, VT, USA) to calculate the cell viability. Cytotoxicity was estimated using Graph Pad Prism 5.01 software (San Diego, CA, USA) by comparing CLO-treated and -untreated cells. The maximal non-cytotoxic concentration was determined as the maximal concentration of the CLO that did not exert toxic effect detected by WST-8.

LDH release assay for cytotoxicity assays

After treatment of the cells with CoCl₂ for 16 hours, cell culture medium was replaced with the one without CoCl₂ and incubated for additional 4 hours. Cytotoxicity was evaluated 4 hours after reperfusion by the extent of the release of LDH. This was achieved with a CytoTox 96 Non-Radioactive Cytotoxicity Assay kit according to the manufacturer's instructions. Briefly, after the cells were treated, 10 µL of lysis buffer (10×) was added to lyse the cells followed by incubation in a humidified chamber at 37°C, 5% CO₂ for 45 minutes. Then the plate was centrifuged at 250 × g for 5 minutes and 50 µL of clear supernatant was transferred into a new 96-well flat bottom plate, 50 µL of reconstituted substrate was added to each well and mixed thoroughly. The plate was covered with foil to protect it from light and incubated at 37°C for 20 minutes, and then 50 µL of stop solution was added and mixed thoroughly. The absorbance was recorded at 490 nm within an hour after the addition of stop solution.

Assays of SOD, ROS, and LPD

SOD was measured according to the instructions provided with the assay kits. ROS was measured as that of H₂O₂ content (Wu et al., 2017). Lipid peroxidation was measured by the TBARS assay that measures malondialdehyde (MDA) level (Yan et al., 1997b). Briefly, for SOD assay, after the cells were subjected to different treatments, they were washed twice with cold PBS on ice. 0.5 mL of ice cold lysis buffer was added and reacted for 10 minutes on ice. Cells or debris were collected with a rubber policeman, and the cell extract was centrifuged at 12,000 × g for 5 minutes. 20 µL of supernatant and 160 µL of working reagent were transferred to each well and mixed, and then 20 µL of diluted xanthine oxidase was added to each assay well quickly. Optical density at 40 nm, OD_{40nm} (OD₀) was read immediately and incubated for 60 minutes at room temperature in the dark, and OD_{440nm} (OD₆₀) was read again. For H₂O₂ and TBARS assays, after the cells were subjected to different treatments, cell lysis buffer was added to each well. The plate was centrifuged and supernatants were collected for the following analysis. For H₂O₂ assay, 40 µL of supernatant was transferred into separate wells of a 96-well plate with clear flat bottom, 200 µL of detection reagent was added to each well, and the plate was incubated 30 minutes at room temperature and OD_{585nm} was read. For TBARS assay, 100 µL of cell lysate was placed into a pre-labeled 1.5 mL micro-centrifuge tube followed by addition of 200 µL of 10% ice cold TCA. The tube was incubated for 5 minutes on ice and then centrifuged at 10,000 × g for 5 minutes. Upon completion of centrifugation, 200 µL of supernatant was transferred to separate tubes, to which 200 µL of TBA reagent was added and mixed. After incubation at 100°C for 60 minutes, each tube was cooled down to room temperature and centrifuged again. OD_{535nm} was read.

Carbonyl-modified protein detection

The carbonyl-modified protein in HT22 cells was measured using an aldehyde/keto-reactive probe and then subjected to western blot assay according to the previously described

method with slight modifications (Wu et al., 2016). In brief, HT22 cells were seeded in 6-well plates at 3 × 10⁵ cells/well in DMEM as described above. Three wells were prepared for each treatment or control. After the cells were subjected to different treatments, they were harvested and rinsed twice with PBS. This was followed by addition of 500 µL Trypsin for 1 minute digestion and DMEM was added to stop the digestion. The liquid was blew repeatedly and transferred into a new Eppendorf tube. After centrifugation (4°C, 1000 × g for 10 minutes), the supernatant was discarded and cells were resuspended in PBS and washed twice, then 200 µL of PBS was added to break the cells using ultrasonication. Following protein quantitation in the cell lysate, an appropriate amount of cell lysate was mixed with incubation buffer (20 mM K₃PO₄, pH 7.4, 1% Triton X-100, 0.5 M EGTA (K⁺), 0.5 M EDTA (Na⁺)) and aldehyde-reactive probe (ARP). ARP-labeled proteins were then separated by 10% SDS-PAGE, and transferred electrophoretically onto polyvinylidene difluoride (PVDF) membranes. Following 1 hour blocking with 5% skim milk, the membranes were washed three times with TBS with 0.01% Tween 20 (TBST) and then incubated with streptactin-HRP conjugate overnight at 4°C. Membrane signals were detected using enhanced chemiluminescence (ECL) western blotting reagent (Bio-Rad) and imaged by BioRad ChemiDoc Imaging System.

Apoptosis assay

Apoptosis was evaluated by caspase-3 assay according to the instructions provided with the assay kits (BioAssay Systems). Briefly, after the cells were subjected to different treatments, the culture media was aspirated from the wells. Then 100 µL of working reagent (containing 100 µL assay buffer, 2 µL substrate, and 2 µL DTT) was added to each well immediately and mixed by shaking the plate for 60 seconds at 100-200 r/min on a plate shaker. The plate was then incubated at 37°C for 60 minutes in the dark. Fluorescence intensity was read by a microplate fluorimeter with excitation at 400 nm and emission at 490 nm.

Statistical analysis

Statistical analysis was performed using Graph Pad Prism 5.01 software (GraphPad Software Inc., San Diego, CA, USA). Data were analyzed by one-way analysis of variance with the Tukey's *post-hoc* test and presented as histograms as the mean ± SD. SPSS 16.0 software (SPSS, Chicago, IL, USA) was used to conduct statistical analysis. Results are expressed as the mean ± SD and the differences among groups were tested with Student's *t*-test. Neurological score was performed using the Mann-Whitney *U* test. Differences were considered statistically significant at *P* < 0.05.

Results

Chemical structure of CLO

The monomeric compounds are light yellow powder, 1% ferric chloride reaction color was yellowish green. ¹HNMR (400 MHz, CD₃OD) δ: 4.94 (1 H, d, *J* = 10.0 Hz, 1-H), 7.50 (1 H, d, *J* = 8.2 Hz, H-6'), 7.54(H, brs, H-2'), 6.89 (1 H, d, *J* =

8.0 Hz, H-5), 6.52 (1 H, s, H-3), 6.26 (1 H, s, H-6); ¹³CNMR (100 MHz, CD₃OD) δ: 184.2 (C-4), 166.7 (C-2), 164.6 (C-7), 162.7 (C-5), 158.1 (C-9), 151.0 (C-4'), 147.1 (C-3'), 124.1 (C-1'), 121.0 (C-6'), 116.8 (C-5'), 115.0 (C-2'), 105.8 (C-8), 105.2 (C-10), 103.7 (C-3), 99.4 (C-6), 83.0 (C-5''), 80.4 (C-3''), 75.4 (C-1''), 72.9 (C-2''), 70.9 (C-4''), 63.3 (C-6''). The above spectrum data and physical and chemical properties are consistent with what was reported in the literature (Li et al., 2008). Therefore, the compound was identified to be orientin (Figure 1).

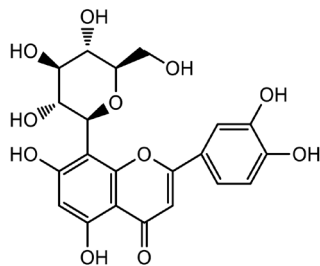


Figure 1 Chemical structure of *Cyperus esculentus* L. orientin.

In vivo studies

CLO increases the neurological score of rats after brain I/R

As shown in Table 1, the symptoms of the body turning to the outside circle were found in the model group, indicating that cerebral ischemia/reperfusion caused obvious neurological deficit. After treatment, neurological function score was significantly lower in the high-dose and low-dose groups than that in the model group ($P < 0.001$), suggesting that oil sedge alcohol extract could attenuate neurological function deficit in rats after focal cerebral I/R injury.

CLO attenuates the brain water content of rats after I/R

As shown in Table 2, there was no significant difference in brain water content in the left hemisphere (non-ischemic side). Compared with the sham operation group, the cerebral tissue water content in the ischemic side (right hemisphere of the brain) of the model group was significantly increased ($P < 0.01$). The brain water content of the high-dose and low-dose intervention groups was significantly lower than that in the model group ($P < 0.01$), suggesting that both the high-dose and low-dose *Cyperus esculentus* L. (30% ethanol eluent) could significantly reduce the brain water content in I/R injury and alleviate the edema in the ischemic side.

CLO attenuates the cerebral infarct volume of rats after I/R

As shown in Table 3, rat cerebral tissue of the sham group had no infarction, and brain tissue on the ischemic side in the model group had a large range of pale infarct area. Compared with the model group, infarct volume was significantly decreased after treatment in the high-dose and low-dose intervention groups ($P < 0.01$ or $P < 0.05$). Therefore, high-dose and low-dose *Cyperus esculentus* L. (30% ethanol eluent) had significant protective effect on cerebral infarction caused by cerebral I/R injury in rats.

Table 1 *Cyperus esculentus* L. orientin increases neurological score of rats at 24 hours after ischemia/reperfusion injury

Group	Score
Sham	0
Model	2.0±0.55 ^{†††}
Positive control 1 (20 mg/kg)	1.42±0.67 ^{†††###}
Positive control 2 (0.3 tablet/kg)	1.33±0.52 ^{†††###}
High-dose intervention (500 mg/kg)	1.25±0.42 ^{†††###}
Low-dose intervention (125 mg/kg)	1.33±0.52 ^{†††###}

$P < 0.001$, vs. model group; ††† $P < 0.001$, vs. sham group. Data are presented as the mean ± SD ($n = 6$, Mann-Whitney *U* Test).

Table 2 *Cyperus esculentus* L. orientin attenuates the brain water content of rats after I/R

Group	Brain water content in the left hemisphere (%)	Brain water content in the right hemisphere (%)
Sham	0.8148±0.0036	81.31 ± 0.0087
Model	0.8186±0.0006	83.42 ± 0.0047 ^{†††}
Positive control 1 (20 mg/kg)	0.8165±0.0009	82.08±0.0050 ^{###}
Positive control 2 (0.3 tablet/kg)	0.8173±0.0015	80.81±0.0020 ^{###}
High-dose intervention (500 mg/kg)	0.8144±0.0018	82.24 ± 0.0053 ^{###†}
Low-dose intervention (125 mg/kg)	0.8154±0.0052	82.25 ± 0.0086 ^{###†}

$P < 0.01$, ### $P < 0.001$, vs. model group; † $P < 0.05$, ††† $P < 0.001$, vs. sham group. Data are presented as the mean ± SD ($n = 6$, one-way analysis of variance followed by Tukey *post hoc* test).

Table 3 *Cyperus esculentus* L. orientin attenuates the cerebral infarct volume of rats after ischemia/reperfusion injury

Group	Cerebral infarct volume (%)
Sham	0
Model	19.23±4.56
Positive control 1 (20 mg/kg)	10.23±3.76 ^{††}
Positive control 2 (0.3 tablet/kg)	15.23±3.85 [†]
High-dose intervention (500 mg/kg)	13.23±4.10 ^{††}
Low-dose intervention (125 mg/kg)	14.93±4.43 [†]

† $P < 0.05$, †† $P < 0.01$, vs. sham group. Data are presented as the mean ± SD ($n = 6$, one-way analysis of variance followed by Tukey *post hoc* test).

In vitro studies

The cytotoxicity of CLO in HT22 cells

To investigate the cytotoxicity of CLO and STO in HT22 cells, cell viability was measured by cell morphology and WST-8 assay. As shown in Figure 2A and B, treatment of CLO and STO for 12 hours had no significant effects on the morphologic changes of HT22 cells and cell viability at the concentrations ranging from 100 to 600 μg/mL ($P > 0.05$).

CLO attenuates CoCl₂-induced I/R injury in HT22 cells

To determine the effects of CLO and STO on CoCl₂-induced HT22 cells after I/R injury, we measured cell viability by cell morphology and WST-8 assay after CoCl₂ treatment, a well-established model for I/R injury (Zheng et al., 2003; Park et al., 2004). As shown in Figure 3A and B, treatment with CoCl₂ (500 μM) for 16 hours and reperfusion for 4

hours markedly reduced HT22 cell viability, and resulted in chromatin condensation compared to the control group ($P < 0.01$). Additionally, incubation with 100–600 $\mu\text{g}/\text{mL}$ CLO and STO for 12 hours attenuated CoCl_2 -induced HT22 cells after I/R injury in a significantly dose-dependent manner.

CLO attenuates CoCl_2 -induced LDH leakage in HT22 cells

To study the effects of CLO on LDH leakage after I/R injury, we measured the level of LDH leakage. After exposure to CoCl_2 , LDH leakage was significantly decreased when compared to that of the control cells ($P < 0.001$) (Figure 4). In contrast, LDH leakage was increased by incubation with CLO (100 and 600 $\mu\text{g}/\text{mL}$) and STO (100, 200, and 400 $\mu\text{g}/\text{mL}$).

CLO increases CoCl_2 -induced SOD activity in HT22 cells

To investigate the effects of CLO on CoCl_2 -induced SOD activity, the activity of SOD in HT22 cells was measured. As shown in Figure 5, exposure of HT22 cells to CoCl_2 markedly increased SOD activity ($P < 0.01$). However, when the cells were incubated with CLO and STO, the activity of SOD increased in different degrees, but there was no statistical significance.

CLO attenuates CoCl_2 -induced hydrogen peroxide production in HT22 cells

To investigate the protective action of CLO against I/R injury, we measured the level of reactive oxygen species. In particular, we measured hydrogen peroxide content as a way of reflecting oxidative stress (Wu et al., 2017). After exposure to CoCl_2 , hydrogen peroxide production was significantly increased when compared to that of the control cells ($P < 0.001$; Figure 6), indicating that CoCl_2 induced oxidative stress in HT22 cells. In contrast, hydrogen peroxide production was decreased by incubation with CLO (400 and 600 $\mu\text{g}/\text{mL}$) and STO (200, 400, and 600 $\mu\text{g}/\text{mL}$) in a dose-dependent manner (Figure 6), demonstrating the antioxidant property of CLO.

CLO decreases CoCl_2 -induced lipid peroxidation in HT22 cells

To investigate the effects of CLO on CoCl_2 -induced lipid peroxidation, the level of MDA in HT22 cells was measured. As shown in Figure 7, exposure of HT22 cells to CoCl_2 markedly increased MDA level ($P < 0.01$). However, when the cells were incubated with CLO and STO, the increase in MDA level induced by CoCl_2 was significantly prevented by STO at 400 $\mu\text{g}/\text{mL}$ ($P < 0.01$). For unknown reasons, CLO did not show significant effects on lipid peroxidation.

CLO attenuates brain water content and cerebral infarct volume in rats after cerebral I/R injury

To investigate the mechanism underlying the neuroprotective effects of CLO, we measured brain water content and cerebral infarct volume. We Longa's neurological deficit score and selected rats scored > 3 , as shown in Table 1. The results are shown in Tables 2 and 3. As shown in Table 1, there was no obvious neurological disorder in the sham group, and the score was 0. The symptoms of the body turning to the outside circle were found in the model group, indicating that

cerebral I/R caused obvious neurological deficits. After treatment, the neurological functional score in the high-dose and low-dose intervention groups was significantly lower than that in the model group ($P < 0.001$), suggesting that oil sedge alcohol extract could attenuate neurological dysfunction in rats after focal cerebral I/R injury.

As shown in Table 2, there was no significant difference in brain water content in the left hemisphere (non-ischemic side) between groups. Brain water content in the ischemic side (right hemisphere) in the model group was significantly increased compared with the model group ($P < 0.01$). Brain water content in the high-dose and low-dose intervention groups was significantly lower than that in the model group ($P < 0.01$), suggesting that both high-dose and low-dose *Cyperus esculentus* L. (30% ethanol eluent) could significantly reduce brain water content after I/R injury and alleviate the edema in the ischemic hemisphere.

As shown in Table 3, cerebral infarction was not observed in the sham group, and in the model group, brain tissue in the ischemic hemisphere had a large range of pale infarct area. Compared with the model group, the infarct volume was significantly shrunk after treatment in the high-dose and low-dose intervention groups ($P < 0.01$ or $P < 0.05$). This indicates that high-dose and low-dose *C. esculentus* L. (30% ethanol eluent) had significantly protective effects on cerebral infarction caused by cerebral I/R injury in rats.

Compared to sham group, pretreatment of CLO decreased dose-dependently brain water content and cerebral infarct volume. These results indicate that CLO can increase neurological deficit score and had neuroprotective effects during cerebral I/R injury.

CLO attenuates CoCl_2 -induced protein oxidation in HT22 cells

We measured protein carbonylation as a parameter for oxidative stress (Zheng et al., 2003; Park et al., 2004). Protein carbonyl content was assessed by western blot assay of ARP-labeled protein samples. Results in Figure 8 demonstrate that CoCl_2 itself induced massive protein carbonyl formation. In the presence of CLO, protein carbonyl intensity showed a dose-dependent decrease. This result indicates that CLO attenuated protein oxidation induced by CoCl_2 .

CLO decreases CoCl_2 -induced elevation of caspase-3 in HT22 cells

Oxidative stress induced neuronal death exhibited features of apoptosis in stroke, and the caspase inhibitor z-VAD-FMK decreased caspase-3 activation, reduced blood-brain barrier permeability, relieved vasospasm, abolished brain edema and improved neurological outcome (Yan et al., 1997a). Thus, caspase-3 was a key component in the execution process of apoptosis (Yan and Sohal, 1998). To determine whether CLO exerts anti-apoptotic effects, caspase-3 assay was performed. An increase in caspase-3 activity is well known to be an indicative of increased cell death (Ouyang et al., 1999; Ko et al., 2005). HT22 cells treated with CoCl_2 resulted in a significant increase in the level of caspase-3 compared to the

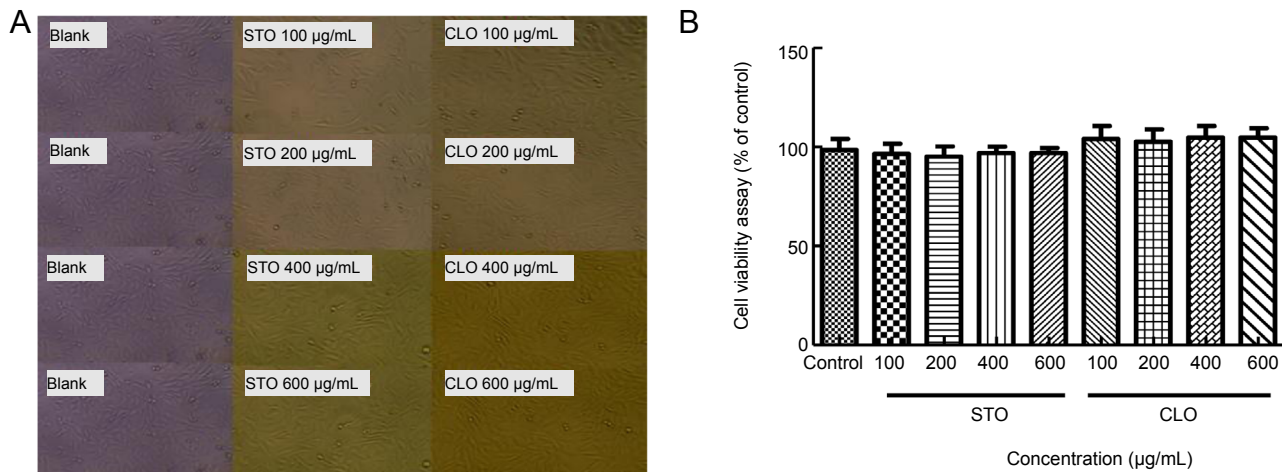


Figure 2 Cytotoxicity of CLO and STO in HT22 cells. (A) The structure of orientin in the leaves of *Cyperus esculentus* L. HT22 cells were treated with different concentrations of CLO and STO alone for 12 hours. (B) Cells were photographed using a photomicroscope (original magnification, 10×). (C) Cell viability was determined by WST-8 assay. Data are presented as the mean ± SD ($n = 3$ independent experiments, one-way analysis of variance followed by Tukey's *post hoc* test). CLO: *Cyperus esculentus* L. orientin; STO: standard orientin.

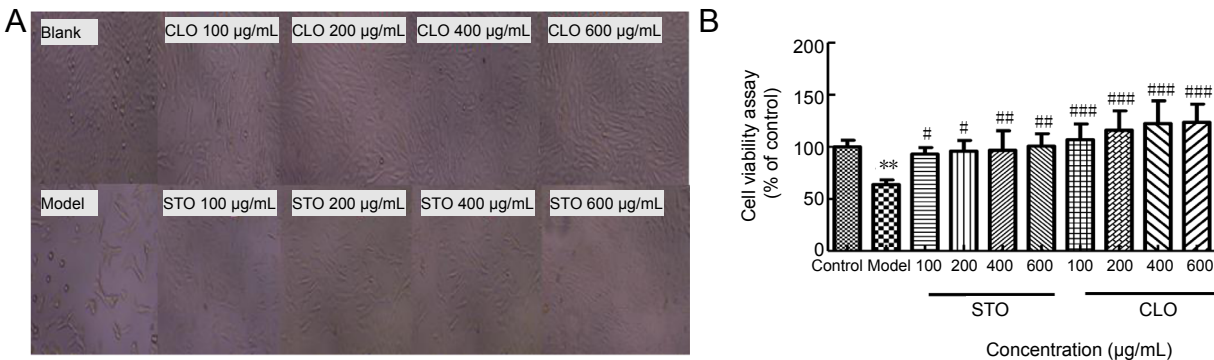


Figure 3 Protective effects of CLO and STO on CoCl_2 (50 µg/mL)-induced cytotoxicity in HT22 cells. HT22 cells were exposed to various concentrations of CLO and STO (100, 200, 400, 600 µg/mL) for 12 hours. After pre-treatment, cells were treated with 500 µM CoCl_2 for 16 hours and then culture medium was removed. Meanwhile, Dulbecco's modified Eagle medium (DMEM) with 10% fetal bovine serum was added and maintained for 4 hours. (A) Cells were photographed using a photomicroscope (original magnification, 10×). (B) Cell viability was determined by WST-8 assay. $**P < 0.01$, vs. control group; $\#P < 0.05$, $\#\#P < 0.01$, $\#\#\#P < 0.001$, vs. model group. Data are presented as the mean ± SD ($n = 3$ independent experiments, one-way analysis of variance followed by Tukey's *post hoc* test). CLO: *Cyperus esculentus* L. orientin; STO: standard orientin.

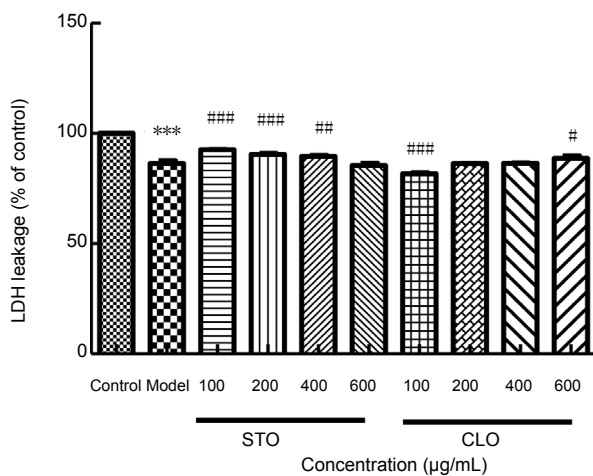


Figure 4 CLO and STO increase CoCl_2 (50 µg/mL)-induced LDH leakage. Cell viability was determined by WST-8 assay. $***P < 0.001$, vs. control group; $\#P < 0.05$, $\#\#P < 0.01$, $\#\#\#P < 0.001$, vs. model group. Data are presented as the mean ± SD ($n = 3$ independent experiments, one-way analysis of variance followed by Tukey's *post hoc* test). CLO: *Cyperus esculentus* L. orientin; LDH: Lactate dehydrogenase; STO: standard orientin.

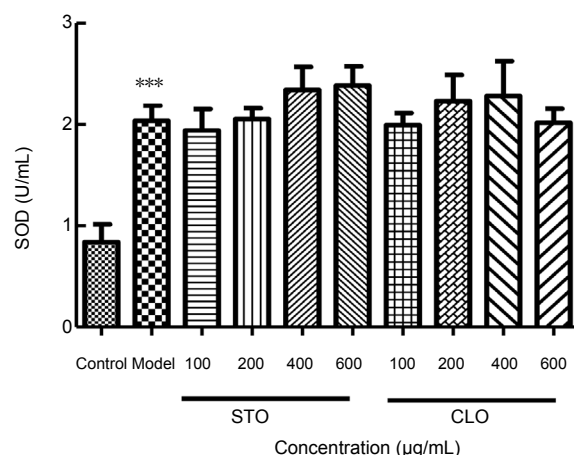


Figure 5 CLO and STO increase CoCl_2 (50 µg/mL)-induced SOD activity. $***P < 0.001$, vs. control group. Data are presented as the mean ± SD ($n = 3$ independent experiments, one-way analysis of variance followed by Tukey's *post hoc* test). CLO: *Cyperus esculentus* L. orientin; SOD: Superoxide dismutase; STO: standard orientin.

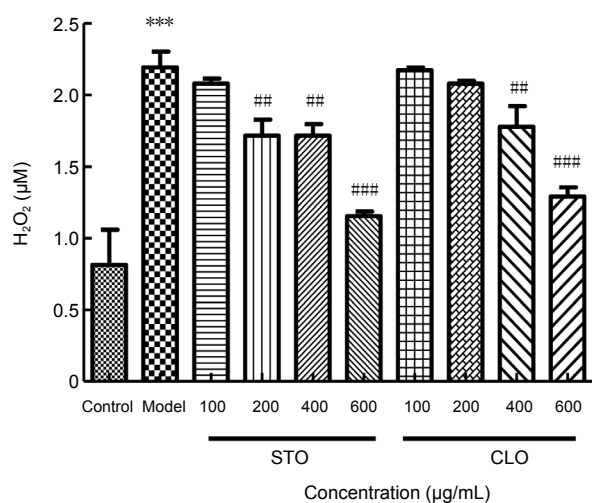


Figure 6 CLO and STO reduce CoCl₂ (50 µg/mL)-induced peroxide production. ****P* < 0.001, vs. control group; ##*P* < 0.01, ###*P* < 0.001, vs. model group. Data are presented as the mean ± SD (*n* = 3 independent experiments, one-way analysis of variance followed by Tukey's *post hoc* test). CLO: *Cyperus esculentus L. orientin*; STO: standard orientin.

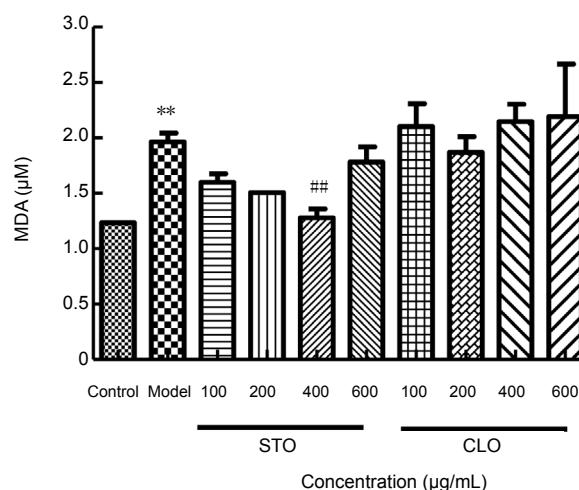


Figure 7 CLO and STO attenuate CoCl₂ (50 µg/mL)-induced change in MDA content. ***P* < 0.01, vs. control group; ##*P* < 0.01, vs. model group. Data are presented as the mean ± SD (*n* = 3 independent experiments, one-way analysis of variance followed by Tukey's *post hoc* test). CLO: *Cyperus esculentus L. orientin*; MDA: malondialdehyde; STO: standard orientin.

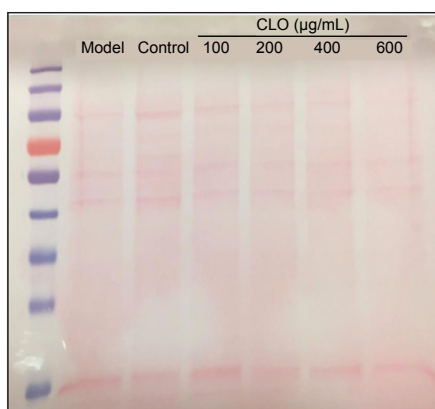
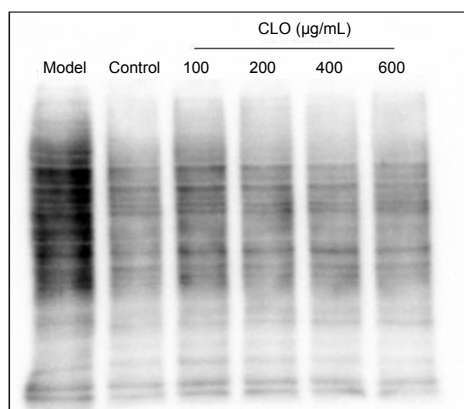


Figure 8 CLO and STO attenuate CoCl₂ (50 µg/mL)-induced protein carbonylation (western blot detection).

Protein carbonyls were labeled by an aldehyde reactive probe as described in the text. Left panel: protein staining by Ponceau red; right panel: Western blot detection of protein carbonylation. CLO: *Cyperus esculentus L. orientin*; STO: standard orientin.

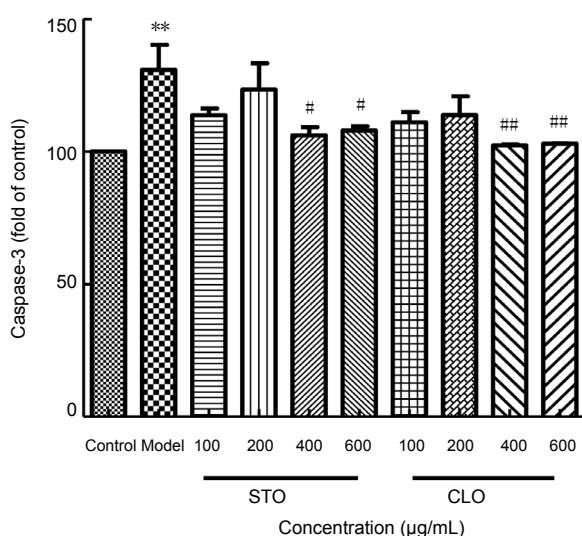


Figure 9 CLO and STO attenuate CoCl₂ (50 µg/mL) -induced change in caspase-3 level. ***P* < 0.01, vs. control group; #*P* < 0.05, ##*P* < 0.01, vs. model group. Data are presented as the mean ± SD (*n* = 3 independent experiments, one-way analysis of variance followed by Tukey's *post hoc* test). CLO: *Cyperus esculentus L. orientin*; STO: standard orientin.

control group (*P* < 0.01; **Figure 9**). On the other hand, both CLO and STO significantly decreased the level of caspase-3 and at the same concentrations (400 and 600 µg/mL), CLO was more potent than STO (**Figure 9**).

Discussion

Overall, our present study showed that CLO attenuated brain water content and cerebral infarct volume in rats after cerebral I/R injury. CoCl₂-induced decrease in cell viability was ameliorated by CLO and CLO itself did not show detectable cytotoxicity at the concentrations tested. Further studies indicate that CoCl₂-induced cell injury involves elevation in oxidative stress reflected by increased H₂O₂ production, enhanced lipid peroxidation, and augmented protein oxidation. However, CLO did not reduce the release of LDH nor increase the activity of SOD, and the reason is unknown, so we will continue to explore its causes in the future. All these oxidative stress parameters except SOD could be attenuated by CLO. Moreover, in the presence of CLO, cell death, assessed by caspase-3 activity, was significantly decreased.

It should be indicated that HT22 cells used in this study

was mouse hippocampal neuronal cell line, while experimental cerebral I/R models were established on the basis of middle cerebral artery occlusion method, which mainly causes I/R injury within the cortex on the operated hemisphere. Therefore, to better integrate the *in vivo* and *in vitro* findings of the present study, primary cortical neurons instead of HT22 cells will need to be investigated in the future and the outcome of primary cortical neuron culture in the presence of CoCl_2 should be compared with that of ischemic stroke.

It should also be pointed out that while our current study was solely focused on animal models and cell cultures, the results could lay foundation for future testing of CLO in humans, where the neuroprotective effects of CLO in stroke patients could be evaluated following comprehensive analysis on the potential toxic effects and risk of CLO in animal models.

Taken together, our present study demonstrates that CLO has neuroprotective effects against cerebral I/R injury. The underlying protective mechanisms of CLO against ischemic injury and CoCl_2 -induced cell death mainly involve decrease in cellular oxidative stress. Our study may provide foundation for future studying CLO as a therapeutic agent in clinical studies.

Acknowledgments: The authors would like to thank Dr. Wen-Jun Li (University of North Texas Health Science Center, USA) for providing the HT22 cells.

Author contributions: SSW, JYZ, JZW, YXT, and YP did experiments and were involved in data collection. SQJ, RMZ, and LJY performed the experiments, interpreted data, and wrote, reviewed and edited the manuscript.

Conflicts of interest: The authors declare that there are no conflicts of interest associated with this manuscript.

Financial support: This work was financially supported by the National Natural Science Foundation of China, No. 31770385 (to SQJ). The funding sources had no role in study conception and design, data analysis or interpretation, paper writing or deciding to submit this paper for publication.

Institutional review board statement: All experimental procedures and protocols were approved on May 16, 2016 by the Experimental Animal Ethics Committee of Xinjiang Medical University of China (approval No. IACUC20160516-57).

Copyright license agreement: The Copyright License Agreement has been signed by all authors before publication.

Data sharing statement: Datasets analyzed during the current study are available from the corresponding author on reasonable request.

Plagiarism check: Checked twice by iThenticate.

Peer review: Externally peer reviewed.

Open access statement: This is an open access journal, and articles are distributed under the terms of the Creative Commons Attribution-Non-Commercial-ShareAlike 4.0 License, which allows others to remix, tweak, and build upon the work non-commercially, as long as appropriate credit is given and the new creations are licensed under the identical terms.

Open peer reviewer: Rong Xie, Department of Neurosurgery, Fudan University Huashan Hospital, China

Additional file: Open peer review report 1.

References

Ayeh-Kumi PF, Tetteh-Quarcoo PB, Duedu KO, Obeng AS, Addo-Osafo K, Mortu S, Asmah RH (2014) A survey of pathogens associated with *Cyperus esculentus* L (tiger nuts) tubers sold in a Ghanaian city. *BMC Res Notes* 7:343.
Chan PH (2001) Reactive oxygen radicals in signaling and damage in the ischemic brain. *J Cereb Blood Flow Metab* 21:2-14.
Chang QY, Lin YW, Hsieh CL (2018) Acupuncture and neuroregeneration in ischemic stroke. *Neural Regen Res* 13:573-583.
Chun HS, Kim JM, Choi EH, Chang N (2008) Neuroprotective effects of several Korean medicinal plants traditionally used for stroke remedy. *J Med Food*

11:246-251.

- Duan ZZ, Zhou XL, Li YH, Zhang F, Li FY, Su-Hua Q (2015) Protection of Mordica charantia polysaccharide against intracerebral hemorrhage-induced brain injury through JNK3 signaling pathway. *J Recept Signal Transduct Res* 35:523-529.
Feng YH, Zhu ZH, Wu CX, Zhou GP (2016) Effects of electroacupuncture at points selected by orthogonal experiment on the extracellular signal regulated kinase signal pathway in a rat model of cerebral ischemia-reperfusion injury. *Zhongguo Zuzhi Gongcheng Yanjiu* 20:5953-5958.
Gao Z, Huang K, Xu H (2001) Protective effects of flavonoids in the roots of *Scutellaria baicalensis* Georgi against hydrogen peroxide-induced oxidative stress in HS-SY5Y cells. *Pharmacol Res* 43:173-178.
Goszcz K, Duthie GG, Stewart D, Leslie SJ, Megson IL (2017) Bioactive polyphenols and cardiovascular disease: chemical antagonists, pharmacological agents or xenobiotics that drive an adaptive response? *Br J Pharmacol* 174:1209-1225.
Jing S, Wang S, Li Q, Zheng L, Yue L, Fan S, Tao G (2016) Dynamic high pressure microfluidization-assisted extraction and bioactivities of *Cyperus esculentus* (C. esculentus L.) leaves flavonoids. *Food Chem* 192:319-327.
Ko CH, Shen SC, Hsu CS, Chen YC (2005) Mitochondrial-dependent, reactive oxygen species-independent apoptosis by myricetin: roles of protein kinase C, cytochrome c, and caspase cascade. *Biochem Pharmacol* 69:913-927.
Li CX, Wang XQ, Cheng FF, Yan X, Luo J, Wang QG (2019) Hyodeoxycholic acid protects the neurovascular unit against oxygen-glucose deprivation and reoxygenation-induced injury in vitro. *Neural Regen Res* 14:1941-1949.
Li S, Cai J, Liu J (2008) Chemical constituents of Chinese globeflower. *Yatai Chuantong Yiyao* 4:18-19.
Li XY, Sun W, Yang Y, Zhang X, Li DM, Wang HZ, Sui XN, Chang H, Teng XH, Hu T, Zhang JB (2018) Multimode computed tomography evaluation of the efficacy and safety of an extended thrombolysis time window (3-9 hours) for acute ischemic stroke: study protocol for a retrospective clinical trial based on medical records. *Asia Pac J Clin Trials Nerv Syst Dis* 3:43-52.
Liu LY, Wang HY, Huang XL (2016) Cardioprotection of orientin against myocardial ischemia reperfusion injury through induction of autophagy. *Zhongguo Yaolixue Tongbao* 32:542-547.
Longa EZ, Weinstein PR, Carlson S, Cummins R (1989) Reversible middle cerebral artery occlusion without craniectomy in rats. *Stroke* 20:84-91.
Ouyang YB, Tan Y, Comb M, Liu CL, Martone ME, Siesjo BK, Hu BR (1999) Survival- and death-promoting events after transient cerebral ischemia: phosphorylation of Akt, release of cytochrome C and activation of caspase-like proteases. *J Cereb Blood Flow Metab* 19:1126-1135.
Park S, Yamaguchi M, Zhou C, Calvert JW, Tang J, Zhang JH (2004) Neurovascular protection reduces early brain injury after subarachnoid hemorrhage. *Stroke* 35:2412-2417.
Pun PB, Lu J, Mochhala S (2009) Involvement of ROS in BBB dysfunction. *Free Radic Res* 43:348-364.
Simoes Pires EN, Frozza RL, Hoppe JB, Menezes Bde M, Salbego CG (2014) Berberine was neuroprotective against an in vitro model of brain ischemia: survival and apoptosis pathways involved. *Brain Res* 1557:26-33.
Su LP, Wang SS, Jing SQ (2017) The preliminary study on microcirculation and the anticoagulation activities of *Cyperus esculentus* L. *Food Industry* 34:46-49.
Tokmak M, Sehitoğlu MH, Yuksel Y, Guven M, Akman T, Aras AB, Yaka U, Gomeksiz C, Albayrak SB, Cosar M (2017) The axon protective effects of syringic acid on ischemia/reperfusion injury in a rat sciatic nerve model. *Turk Neurosurg* 27:124-132.
Weseler AR, Bast A (2012) Pleiotropic-acting nutrients require integrative investigational approaches: the example of flavonoids. *J Agric Food Chem* 60:8941-8946.
Wu J, Jin Z, Yan LJ (2017) Redox imbalance and mitochondrial abnormalities in the diabetic lung. *Redox Biol* 11:51-59.
Wu J, Luo X, Jing S, Yan LJ (2016) Two-dimensional gel electrophoretic detection of protein carbonyls derivatized with biotin-hydrazide. *J Chromatogr B Analyt Technol Biomed Life Sci* 1019:128-131.
Xia X, Cao J, Zheng Y, Wang Q, Xiao J (2014) Flavonoid concentrations and bioactivity of flavonoid extracts from 19 species of ferns from China. *Ind Crops Prod* 58:91-98.
Yan LJ, Levine RL, Sohal RS (1997a) Oxidative damage during aging targets mitochondrial acetylase. *Proc Natl Acad Sci U S A* 94:11168-11172.
Yan LJ, Lodge JK, Traber MG, Packer L (1997b) Apolipoprotein B carbonyl formation is enhanced by lipid peroxidation during copper-mediated oxidation of human low-density lipoproteins. *Arch Biochem Biophys* 339:165-171.
Yan LJ, Sohal RS (1998) Mitochondrial adenine nucleotide translocase is modified oxidatively during aging. *Proc Natl Acad Sci U S A* 95:12896-12901.
Yang T, Li D, Liu F, Qi L, Yan G, Wang M (2015) Regulation on Beclin-1 expression by mTOR in CoCl_2 -induced HT22 cell ischemia-reperfusion injury. *Brain Res* 1614:60-66.
Zhang R, Xu M, Wang Y, Xie F, Zhang G, Qin X (2017) Nrf2-a promising therapeutic target for defending against oxidative stress in stroke. *Mol Neurobiol* 54:6006-6017.
Zheng Z, Zhao H, Steinberg GK, Yenari MA (2003) Cellular and molecular events underlying ischemia-induced neuronal apoptosis. *Drug News Perspect* 16:497-503.

P-Reviewer: Xie R; C-Editor: Zhao M; S-Editor: Li CH; L-Editor: Song LP; T-Editor: Jia Y